PHILOSOPHICAL TRANSACTIONS OF THE ROYAL SOCIETY A MATHEMATICAL, PHYSICAL & ENGINEERING SCIENCES

Dielectric polarization, electrical conduction, information processing and quantum computation in microtubules. Are they plausible?

J. A. TuszyD ski1, J. A. Brown and P. Hawrylak

Phil. Trans. R. Soc. Lond. A 1998 **356**, 1897-1926
doi: 10.1098/rsta.1998.0255

The Royal Society

Dielectric polarization, electrical conduction, information processing and quantum computation in microtubules. Are they plausible?

By J. A. Tuszyński[1], J. A. Brown[1] and P. Hawrylak[2]

[1]*Department of Physics, University of Alberta, Edmonton, Alberta, Canada T6G 2J1*

[2]*Institute for Microstructural Studies, National Research Council, Ottawa, Ontario, Canada K1A 0R6*

The multitude and diversity of functions performed by the cytoskeleton of eukaryotic cells poses a major scientific puzzle. Microtubules, which are the main components of the cytoskeleton, are engaged in such important activities as material transport, cell motility, cell division, signal transduction and possibly information processing within axons of nerve cells. The latter aspect has been recently brought to the forefront of consciousness studies by R. Penrose and S. Hameroff. In this paper we discuss the potential of microtubules as information processing units from a physical standpoint. In particular, since electric dipoles are a characteristic property of protein molecules, and as such may undergo various ordering phase transitions, it can be expected that microtubules support the existence of various ferroelectrically ordered states. It is also argued that the piezoelectric effect may link electric and elastic properties of a dielectric polymer system and hence explain a number of experimental observations both *in vitro* and *in vivo*. Furthermore, preliminary results are shown of recent quantum mechanical calculations for the electrical conduction properties of microtubule protofilaments which support the assertion that the latter may function under certain conditions very much like semiconducting devices. Indirect evidence links the cytoskeleton with information processing and cognitive function. We discuss some plausible ways in which axonal microtubules can be involved in the functioning of the brain. Finally, we present a hierarchy of energy values for a number of physical and chemical interactions of interest and discuss their relative importance.

Keywords: microtubules; quantum computing; electrical conduction; neurotransmitter release; signal propagation; dielectric polarization

1. What are microtubules and what do they do in the cell?

The physical and chemical design underlying the complex multifunctional behaviour of the cell's cytoskeleton is one of the most intriguing unsolved problems of molecular biophysics. The cytoskeleton comprises actin, intermediate filaments, microtubules and centrioles (which, in turn, also contain bundles of microtubules). Microtubules (MTs) are ubiquitous in eukaryotic cell biology and they perform an astounding array of functions in addition to sustaining the structural architecture of the cytoplasm (Dustin 1984). These are (a) material transport of organelles via motor proteins; (b)

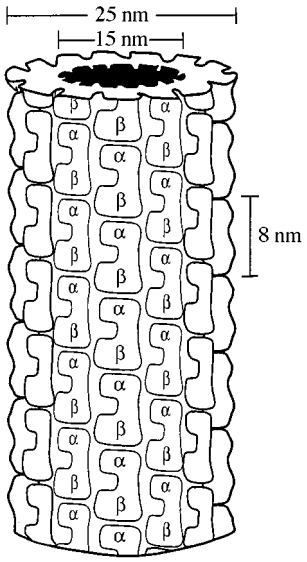

Figure 1. A typical microtubule consisting of 13 protofilaments (vertical columns) Dimensions are indicated. Note the hollow interior and helical packing of tubulin dimers.

cell motility through cilia and flagella; (c) chromosome separation during mitosis; (d) signal transduction within axonal MTs; and most recently discovered (e) a role in the communication between the exterior of the cell and the nucleus (Glanz 1997; Maniotis *et al*. 1997).

Microtubules are hollow cylinders with a 25 nm outer and 15 nm inner diameter (see figure 1) which are formed in the process of polymerization of tubulin protein. Each tubulin molecule is a dimer composed of two highly homologous monomers called α-tubulin and β-tubulin, respectively. The length of each dimer is approximately 8 nm, the width 5 nm and the thickness also 5 nm. These dimers assemble themselves into protofilaments which number 13 almost without exception *in vivo*, although *in vitro* experiments indicate various deviations from the rule to be quite common.

In non-dividing cells, almost all MTs emanate from a centrosome but their individual length constantly varies in a process referred to as *dynamic instability*. In a dividing cell, the above phenomenon is used to form mitotic spindles, which grow at first randomly from the two oppositely positioned centrosomes to eventually anchor themselves to chromosomes and pull the latter apart in the final mitotic phase. During the stable state of a cell, MTs serve as tracks for the transport of vesicles and organelles mediated by various types of motor proteins. In neurons, vesicles are moved along MTs towards synapses by motor proteins.

Two distinct crystal lattices have been seen to form the MT structure and have become known as the A-lattice and the B-lattice (Chrétien & Wade 1991; Amos 1995). The A-lattice with 13 protofilaments is the only lattice without a seam where protofilaments run parallel to the MT axis (figure 2). The assembly and disassembly processes of MTs have been extensively studied over the past two decades both *in vivo* and *in vitro* (Mitchison & Kirshner 1984; Horio & Hotani 1986; Bayley *et al*. 1990; Mandelkow & Mandelkow 1995). The development of a single microtubule passes

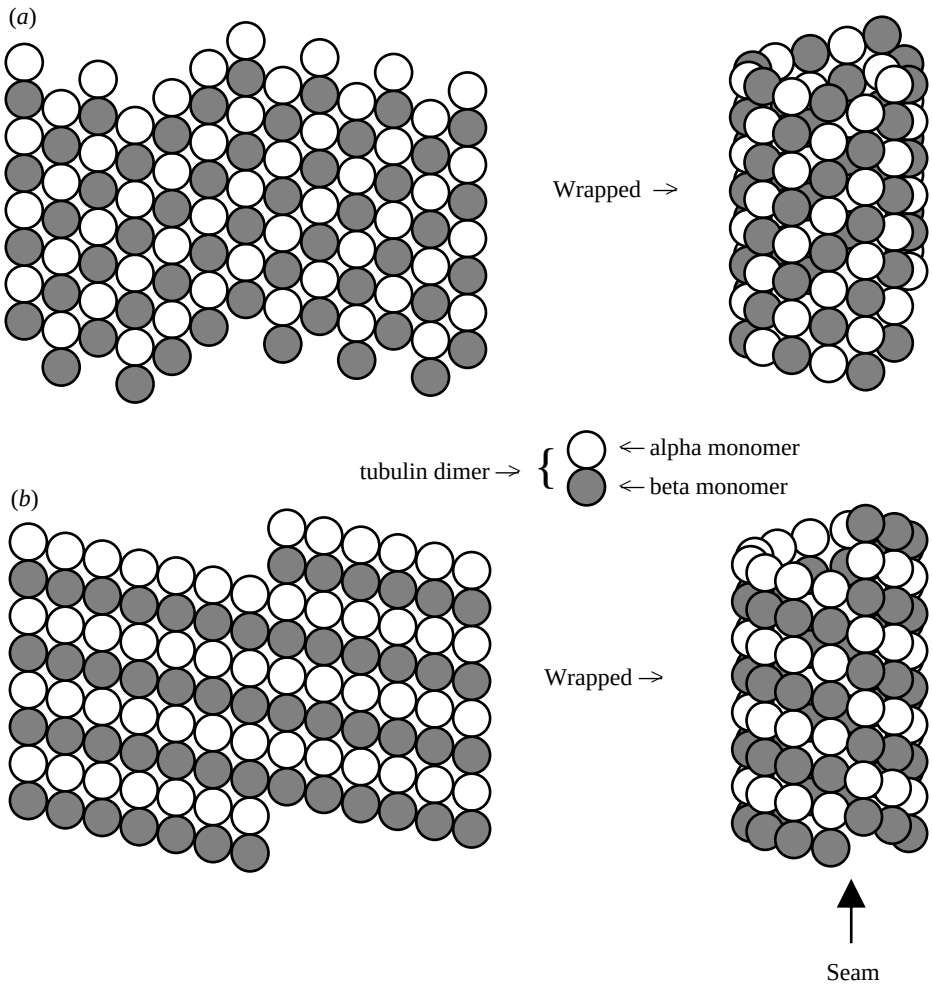

Figure 2. The A and B microtubule lattices: (*a*) the A-lattice exhibits perfect helical symmetry; (*b*) the B-lattice has a structural discontinuity known as a seam.

through several stages starting with a nucleation phase from seed oligomers or microtubule organizing centres (MTOCs) and requiring the presence of γ-tubulin (Sunkel *et al*. 1995). This slow, gradual process eventually reaches an asymptotic density of MT ends and is followed by an almost continuous growth stage which is randomly interrupted by a sudden and catastrophic disassembly followed by another regrowth stage. The ratio of guanosine 5′-triphosphate (GTP) to guanosine 5′-diphosphate (GDP) concentrations in solution determines whether or not and at what rate MTs elongate from a steady-state condition (Engelborghs & Van Houtte 1981). The modelling of MT assembly and disassembly processes *in vitro* as well as *in vivo* through the use of the sophisticated master-equation formalism based on the known chemical reactions and their rates has provided a very accurate and reliable analysis (Flyvbjerg *et al*. 1994). It should be emphasized in this context that MT assembly is a non-equilibrium phenomenon driven by the supply of energy-giving GTP molecules

since only the GTP-tubulin complex is capable of binding to a microtubule. Furthermore, Raman spectroscopy studies revealed that following binding to an MT, GTP attached to the exchangeable site on a tubulin dimer rapidly hydrolyses to GDP, imparting its energy to an unknown destination on the MT lattice. This picture is believed to apply to all but the top layer (or two) of tubulin dimers which have been speculated to form a so-called lateral cap that is required to prevent disassembly.

It is also noteworthy that 'the geometry' of growing MTs (straight protofilaments) differs from that of shrinking ones (curved protofilament ends). This is a direct result of the conformational change that tubulin undergoes upon GTP hydrolysis (Howard & Timasheff 1986). The breaking of lateral bonds first is also consistent with close to a two order of magnitude difference between the elasticity moduli along the axis versus about the circumference in a stable MT; the former being greater.

Finally, it should be mentioned that various types of defects are not uncommon, especially *in vitro*. The number of protofilaments may vary between 12 and as many as 17. MTs often exhibit internal vacancies, breakage points and line defects (Mandelkow & Mandelkow 1994). *In vitro* assembly initially involves a two-dimensional sheet which ultimately closes to form a cylinder and may continue growing as a sheet with the seam closing up behind the growth front. Some researchers claim that the closing of the sheet acts as a trigger for disassembly (Chrétien *et al*. 1995). These problems are almost non-existent *in vivo* where MTOCs provide a template for growth of MTs and MAPs provide additional stabilizing agents (Amos 1995).

We should also add that MTs are highly sensitive to the ionic environment, temperature, pH levels and a number of specific chemicals which bind to their surfaces. For example, Ca^{2+} ions promote disassembly of MTs by enhancing the catastrophe rates (O'Brien *et al*. 1997). The dynamics of MT polymerization are dramatically altered through the use of the drugs: vinblastine (Dhamodharan *et al*. 1995), taxol (Klauber *et al*. 1997) and colchicine (Skoutias & Wilson 1992). An increase in the value of pH of the solution causes an increase in the critical concentration of tubulin for MT formation (Audenaert *et al*. 1989). It has been demonstrated recently that high osmotic pressure in the order of MPa reduces the rate of MT assembly (Barthou *et al*. 1997). All of the above findings are of potential importance in devising new cancer therapies due to the crucial involvement of MTs in the cell division process.

Finally, in this introductory section we should comment on the structure of the constituent protein, tubulin, which has just been resolved at an atomic level (Downing 1998). The development of tubulin appears to be an early evolutionary achievement and a relatively small diversity in the structural isotypes in various species has been found. In a given organism, isotypes of α- and β-tubulin have been found to correlate to some degree with the function performed by the corresponding microtubule, although in some cases isotypes may be interchangeable (Joshi & Cleveland 1990). There are known to be six isotypes of α- and seven of β-tubulin in humans. What complicates the issue of linking structure with function is the plethora of post-translational modifications of tubulin which include phosphorylation, acetylation, detyrosination and glutamylation. It is interesting to note that the greatest divergence among tubulin isotypes is localized to a variable domain called the C-terminus, which is a quasi-linear protrusion from the protein surface containing at least 16 residues (Downing 1998) and possessing a net charge which depends on the solution's pH (Sackett 1997). We believe that this is closely linked to the dipolar properties of microtubules and their role in MTs as carriers of signals. In the next

section we take a closer look at the possibility of ordered dipole phases decorating the surface of a microtubule.

2. Can microtubules be ferroelastic?

Since MTs are protein polymers, there is reason to believe that they are dipolar in character and consequently should be sensitive to electric fields and their gradients. Calculations of electric multipole contributions for a number of proteins have been performed, and the dipole moments found for globular proteins similar in size to tubulin would appear to indicate the existence of a dipole moment in the order of 10^{-27} Cm (Nakamura & Wada 1985; Schlecht 1969). The dipole moment is directly related to each of the peptide groups. Residues of the peptide groups may be either protonated or deprotonated giving rise to a possible net charge on the helix.

According to Sackett (1997) the net charge on a tubulin dimer is pH dependent, being positive at low pH values and highly negative at high pH values. At physiological pH, eight negative charges are expected to exist, which reside mainly in the C-terminus region. Of course, in solution these charges are surrounded by counterions forming a dipolar zone whose thickness corresponds to the Bjerrum length and is of the order of 1 nm at room temperature. If this picture is even approximately correct, it would offer some very attractive possibilities, such as: dipolar orientation predominantly along the protofilament axis, relatively easy to create dipole oscillations, sensitivity to the pH and contents of the solution, cooperative effects, sensitivity to electric fields and their gradients, coupling between elastic deformation and the dipole moment (the piezoelectric effect), etc. Many of the above effects have been experimentally observed and we briefly list them below.

It was suggested a long time ago that bioelectric fields may act to orientate various growth-guiding filaments in the cell (Jaffe & Nuccitelli 1977). Indeed, rearrangement of the cytoskeleton and nuclear transfer was seen in *Tetrahymena thermophila* cells fused by electric fields in the range 300–900 V cm^{-1}. Pronounced effects of electric fields in the 10^3 V m^{-1} range on MTs and actin stress fibres in the fibroblast were observed where filament elongation took place perpendicular to the field gradient and a weakening parallel to it (Harris *et al*. 1990). A possible explanation involves Ca^{2+} influx charges which have been known to be sensitive to low-frequency (3–75 Hz) and low-amplitude electric fields ($E > 10^{-2}$ V m^{-1}) (Berg 1995). Unfortunately, there is only scant evidence indicating direct response of MTs to both electric and magnetic fields. Vassilev *et al*. (1982) observed alignment of MTs in parallel arrays due to the application of both electric and magnetic fields. Electric field intensities used were relatively low, in the range of 20–50 V m^{-1} and were of a pulsed shape. The magnetic field intensity applied was 0.02 T. Similarly, DC electric fields of magnitude 20 V m^{-1} applied in regenerating *Mongeotia* protoplasts resulted in the ordering of MTs (White *et al*. 1990).

If MTs are capable of ordering their dipoles into a ferroelectric state, as we try to argue in this section, this would not be an unusual situation among biopolymers. Indeed, the electret state of most hydrated biopolymers has been found to be a general property of these systems (Fukada 1974). Moreover, bound water was found to strongly contribute to dielectric polarization of biomolecules in solution. Nonlinear effects in transport and polarization storage were discovered which depend on hydration. The nonlinear bioelectret may stimulate ferroelectric hysteresis curves which

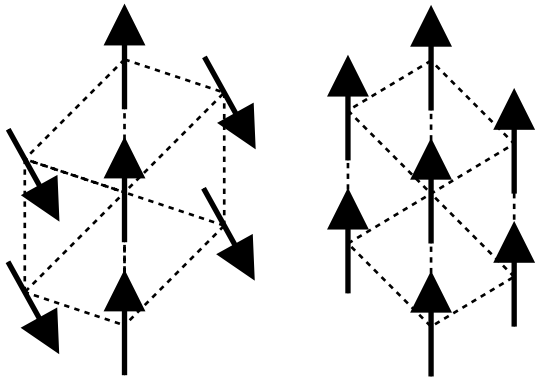

Figure 3. The nearest neighbours of each dimer are arranged as shown in the following diagram. Along the protofilament, parallel alignment is preferred so that the negative heads are close to the positive tails. Between protofilaments, the preferred orientation is determined by the vertical offset between the neighbouring protofilaments.

introduce both memory and irreversibility to the behaviour of these systems (Mascarenhas 1974). Fukada (1974) reported that DNA and RNA are bioelectrets in their hydrated state with a polarization storage as high as 10^{-4} C m^{-2} at fields as low as 100 V m^{-1}. Polarization storage varies drastically with the hydration level, indicating the role of bound water in creating an ordered dielectric state of the complex.

The dielectric constant has a nonlinear dependence upon the protein concentration; this has been linked to the existence of local order in protein molecular assemblies. This is indicative of positional ordering of elongated molecules with permanent dipole moments and it could lead to liquid crystalline properties as well as to molecular electric fields of the order of 10^4–10^5 V m^{-1} in solutions with protein concentrations of the order of 100 mg mL^{-1} (Post 1995).

In our modelling of dipolar properties of MTs our working assumption was that each tubulin dimer possesses a dipole moment $\boldsymbol{p} = Q \cdot \boldsymbol{d}$, where Q is the net charge capable of transfer over distance d. We have also assumed that the projection of the dipole moment on the protofilament axis can only be $+p$ or $-p$ due to strong anisotropy which constrains the mobile charge to only two locations in the dimer. We chose these locations to correspond to the central region in an α- and β-monomer, respectively (Tuszyński *et al*. 1995). The interaction energy between the neighbouring tubulin dimers, labelled i and j, was taken to be of the standard dipole–dipole form:

$$E_{ij} = \frac{1}{4\pi\epsilon\epsilon_0}\frac{3\cos^2\theta - 1}{r_{ij}^3}p^2, \tag{2.1}$$

where ϵ_0 is the permittivity of the vacuum, ϵ is the dielectric constant of the medium, r_{ij} is the distance between sites i and j and θ is the angle between the dipole axis and the direction joining the two neighbouring dipoles (see figure 3).

As stated earlier, we assume that the electric dipole of the tubulin dimer has two possible orientations depending on the conformational state of the molecule. One orientation of the dipole points along the protofilament axis; this is the *up* state. We have some freedom to choose the direction of the dipole in the *down* state since the electric dipole has not been measured in each of tubulin's conformational states. We

have chosen a direction which is roughly opposite to the direction of the *up* state but which is 29° from the vertical and points out away from the MT. This choice is based on the geometry of MT ends which are splaying apart and of tubulin oligomer rings. Our simulations have been carried out with both the tilted and non-tilted down states for comparison. Note that some degree of tilting is necessary for axonal MTs if action potentials are to influence the dipole dynamics.

However, from the dipole interaction point of view, the lattice type is crucial. In the B-lattice, dimers are aligned in nearly horizontal rows. As a result, there is a strong interaction between neighbouring dimers which favours opposite dipole orientations. In the A-lattice, the neighbouring dipole is shifted vertically such that identical orientation of the dipoles is favoured. In either case, there is a strong interaction along individual protofilaments which favours similarly orientated dipoles. The effect of the dipole interactions is that the lattice of *up* and *down* dipoles will self-organize into an energetically favourable configuration. It can be easily predicted that at high temperatures, the lattice has a random state—each individual dimer can be found in the *up* or the *down* state in a rather arbitrary fashion. At lower temperatures, the interaction energy dictates the dipole arrangement and the lattice becomes ordered. The key question is in what temperature range is the the resultant phase transition from dipolar order to disorder to be expected? The answer crucially depends on the choice of as yet largely unknown physical parameter values.

There are two numbers which are put into the model by hand. One is the relative permittivity of tubulin, or more precisely that of tubulin in cytosol, ϵ. As an approximation, we are using the value 10. The dynamics of the model are unaffected by the choice of ϵ but it scales with temperature. Larger values of ϵ reduce interaction strengths and thereby act like a temperature increase. The other number which is put in by hand is the dipole strength of the conformational states of tubulin. We have chosen the dipole magnitude, p, by considering the corresponding dipole charge to be an elementary charge in magnitude and the charge separation to be 4 nm which is the monomer spacing. This gives a value of $p = 192$ Debye which is comparable to the measured dipole moments of some other protein molecules.

The simulations show that a highly ordered phase exists for both the A- and B-lattices at low temperatures. Whether the MT is ordered at physiological temperature depends critically upon p and ϵ since these parameters determine the transition temperature from disorder to order. In the MT A-lattice with 13 protofilaments, we have found a transition temperature of 105 K and in the MT 13B-lattice, the corresponding transition temperature is 218 K. In the case where the *down* state is directly opposite to the *up* state (the non-tilted case), the corresponding transition temperatures are somewhat higher: 160 K for 13A and 248 K for 13B. This shows that the existence of a transition to order is quite robust but that the transition temperature is sensitive to the specific choice of the *down* dipole. All of these temperatures are below human physiological temperature (310 K, 37 °C) but all have been derived based upon our estimates of the dipole moment, p, and the electric permittivity, ϵ:

$$T_{\mathrm{c}} = T_{\mathrm{c}}^{0}\left(\frac{p}{p_0}\right)^{2}\left(\frac{\epsilon_0}{\epsilon}\right). \tag{2.2}$$

This equation demonstrates the scaling of the transition temperature, T_{c}, in a MT which is not subject to electric fields. The values p_0 and ϵ_0 are the values which we have estimated, while p and ϵ are the actual values of the dipole moment and

permittivity of tubulin. The scaling is more complicated in the presence of electric fields. The transition temperature scales directly with the square of p, and inversely with ϵ. Hence, if the dipoles are twice as large as our estimate then the transition temperature would be raised by a factor of four. Should the permittivity be half as large as estimated, the transition temperature would double. The main result is that the MT could easily exist in an ordered state at physiological temperatures without the application of external fields provided $p^2/\epsilon_r > 10\,800\,\text{Debye}^2$. Our original estimate of p^2/ϵ_r was about $3600\,\text{Debye}^2$ which comes within a factor of three of what the model requires. We are hopeful that an experimental value for the dipole moment of tubulin will soon be available or a better estimate arrived at using the latest atomic resolution map of tubulin (Downing 1998).

For modelling purposes, in both lattice types the effective Hamiltonian has been represented as a two-dimensional Ising model (Yeomans 1992) on an appropriate triangular lattice whose interaction constants have been calculated based on the geometry of the lattice chosen:

$$H = -\sum_{\langle nn \rangle} J_{ij} S_i^z S_j^z, \tag{2.3}$$

where S_i^z are dipole projection values on the z-axis which can be either $+1$ or -1. The application of an axial electric field, E, along the length of the MT may serve to order the MT at higher temperatures than without an external field and the effective Hamiltonian becomes

$$H = -\sum_{\langle nn \rangle} J_{ij} S_i^z S_j^z - p \sum_i E S_i^z, \tag{2.4}$$

where p is the magnitude of the dipole moment.

Our simulations suggest that for the 13A-lattice, the electric field starts to be effective at the range 10^4–$10^5\ \text{V m}^{-1}$. This is because at these fields the potential energy $-pE$ becomes of the order of magnitude of the dipole–dipole interaction energies. These values of the electric fields are at least three orders of magnitude larger than those reported by Vassilev *et al.* (1982) as being used in their experiments on aligning MT assemblies. On the other hand, such strong electric fields may be supported across cell membranes. While the effect of the electric field is quite dramatic in the MT 13A-lattice, for the 13B-lattice the effect is greatly reduced because the orientation of the ground state is not ferroelectric. The dipolar ordering is also affected by the binding of microtubule-associated proteins (MAPs). The influence of MAPs was studied for three different superhelical patterns that attached MAPs formed on a MT. An assumption was made that MAPs prevent the dipoles on the tubulin dimers to which they bind from flipping. MAPs enhance the number of dipoles that point in the same direction as the dipole on the MAP tubulin.

Of the three types of cytoskeletal polymers (actin filaments, intermediate filaments and microtubules), it is the two polar structures which participate in material transport (including axonal transport) and cell motility through the use of their respective motor proteins. It is tantalizing to speculate that it might be this polarization which is responsible for guiding the motor proteins, kinesin and dynein, which travel along the MT in opposite directions (Audenaert *et al.* 1989; Barthou *et al.* 1997). It would immediately explain why the transport would be so efficient because collisions would not occur. The motor proteins would simply have to bind preferentially to a particular conformational state of tubulin. The kinesin and dynein protein motors may

be sensitive to the dipole moments of the tubulin molecules on which they step. An ordered lattice would allow for the efficient transport of material along the lattice. For example, if the lattice were ordered in the same way as the MT 13B-lattice, where alternating protofilaments have opposite dipole orientations, one motor might follow the first, third, fifth, etc., protofilaments while the other would follow the second, fourth, sixth, etc., protofilaments.

3. Can axonal MTs propagate secondary signals?

Neurons have a specialized structure and function. Many of the resources of the cell are spread out in the axons which may project for distances greater than 1 m from the cell body. The cytoplasm within the axon is distinct from that in the cell body. It is generally free of organelles, and filled with microtubules and neurofilaments. These filamentous proteins are arranged parallel to the axon, each neuronal MT being typically about 100 μm long, thus spanning more than 10^5 tubulin subunits. The network of cytoskeletal tubes is interconnected by high molecular weight proteins known as MAPs. Their precise function is not understood but tubulin dimers coassembled with MAPs *in vitro* are polymerized more easily and are more stable than MTs assembled from tubulin in the absence of MAPs (Mandelkow & Mandelkow 1995). The MTs of the axon have uniform polarity and lie with their positive ends distal to the cell body (Baas *et al*. 1988; Baas & Black 1990). Once the axonal MTs have been assembled, they are post-translationally modified and their properties are changed. These changes to the MTs cause them to become more stable (Li & Black 1996; Pryer *et al*. 1992). The post-translational post-MT assembly change has also been frequently studied in the last decade. The transition from newly synthesized tubulin to detyrosinated tubulin within a MT can be used to estimate the age of an individual MT.

Greater stability allows the neuronal MTs to participate in other cell activities. Information processing (Hameroff 1987; Tuszyński *et al*. 1995) and energy transport (Satarić *et al*. 1993) have been proposed as secondary MT functions. Consider the central theme of biology in which DNA codes for functional proteins. Now, not only is the tubulin which makes up neuronal MTs specific to humans, but it is also specific to nerve cells and is known to be post-translationally modified. The highly specialized nature of the functional proteins suggests that it has been selected to perform a very specific function which we conjecture may be signal transduction.

Hameroff *et al*. (1988) have introduced a cellular automaton model where a discrete charge is associated with each tubulin dimer and can either be localized in the top monomer (α state) or bottom monomer (β state). The MT lattice of dimers in their α or β states has then been considered as a binary biological computer. The Hameroff model (Hameroff *et al*. 1988) found that signals introduced onto the MT 13A-lattice would propagate along protofilaments. The propagation was either bidirectional or unidirectional depending upon the choice of flipping force thresholds and whether they were symmetric or not. The model also admitted the possibility of signals which periodically flipped back and forth between α and β states but did not move along the protofilaments. The moving patterns of defects were named gliders and the non-propagating defects were called blinkers. The other feature of the Hameroff model was its ability to filter input signals. Some would propagate, others would be modified and would subsequently propagate, and still others would be annihilated. Thus, the

cellular automaton model accepted certain patterns and rejected others. The first modification introduced in our work (Brown & Tuszyński 1997) was simply to replace the discrete charges with dipoles as motivated by our earlier discussion in this paper. Some arbitrary torque threshold was required akin to the force threshold of the original model. Despite the relative weakness of dipole interactions, most of the original features of signal transduction were still present in the modified model. The one difference was a shift in the direction of signal propagation from the N–S direction (along the protofilament) to the NW–SE direction (around the helix).

The lattice dynamics were simulated using a standard Monte Carlo technique (Binder 1988). For a given time-step, the energy of the present state and of the opposite state were calculated. Whether a change of state occurs is a random event whose probability is determined by the availability of stored lattice energy, the temperature, and the threshold to reaction. An important additional feature of the model is the removal of the unphysical flip-flop of states which plagued our early attempts at modelling this system. This is removed by forbidding nearest neighbours from both changing states in the same time-step. Thus, when the dipole interaction favours paired dipoles and the current state of the neighbouring dipoles is *up–down*, in the next time-step they may be *up–down* (unchanged), *up–up* or *down–down* but not *down–up*. When a dipole flips, the change in conformational energy is either removed from or added to the lattice at that location. After the evolution step, energy diffuses to neighbouring sites. Our simulations have been carried out with a diffusion constant which is isotropic and small enough that several time-steps are required for localized energy to dissipate. Energy is conserved by the lattice in our current model; none of the energy is returned to the surrounding medium. It is important to note in this context, that the conformational state of tubulin is not coupled to GTP hydrolysis. These two events are separate but GTP hydrolysis can easily induce the conformational change. Some authors have directly linked these two events and on occasion have proposed the opposite causality, that the conformational change of tubulin induces GTP hydrolysis (Chrétien *et al*. 1995).

Consider the interaction of a MT lattice with an action potential, in which a signal can be identified as a particular sequence of antialigned dipoles on an otherwise well-ordered lattice. Associated with this signal or defect is some additional energy which is recovered when the antialigned dipole falls back to its original configuration (see figure 4). The energy may diffuse in all directions so with six nearest neighbours a single defect is not likely to cause neighbouring dipoles to flip since they receive only about a sixth of the required energy. However, a larger defect such as a group of three or more dimers might successfully maintain its integrity. This has been observed in our model; larger defects have larger lifetimes.

The interesting question is: how does the MT respond to the presence of defects on the ordered lattice? A defect could arise by GTP hydrolysis to GDP at the exchangeable site upon addition of an additional tubulin subunit or by the less frequent hydrolysis of GTP at the non-exchangeable site (Semenov 1996). In either case, the energy released might go into changing the conformation of the molecule and its electric dipole. We no longer observe the smooth propagation of signals along the MT unless some additional mechanism is added to the model. There is nothing to direct the propagation of the defect so it takes a random walk about the MT and dissipates its energy. The efficient propagation of signals could be restored by several mechanisms. Such mechanisms include (i) the application of an external

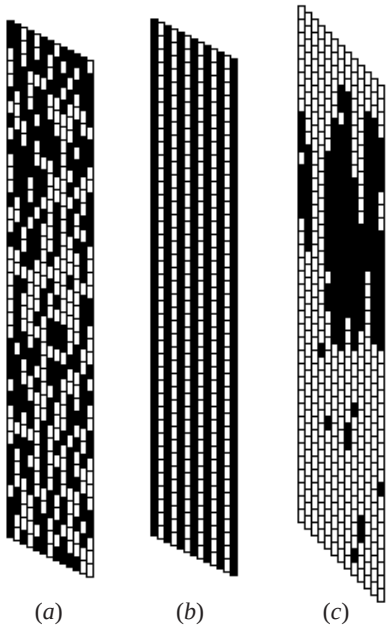

Figure 4. Portions of three MTs are shown. Light boxes represent the 'up' state and dark boxes the 'down' state: (*a*) above the critical temperature of the B-lattice there is disorder; (*b*) below the critical temperature there is spontaneous ordering; (*c*) below the critical temperature of the A-lattice, a large defect (signal) has been introduced. Smaller thermal defects also dot the structure.

field which would bias signal propagation; (ii) an asymmetry in the dipole structure which simply makes it more favourable to propagate in a particular direction; or (iii) mechanical stress if dipoles are coupled to a lattice distortion. The second mechanism could be the result of the bonding between tubulin dimers. If the energy deposited by a dipole flip is comparable with the vibrational energy of a particular bond, it is most likely that this energy would be propagated in that direction. The third mechanism would be the result of a piezoelectric effect, which will be discussed in the next section. There could also be some sort of refractory period which prevents the retrograde propagation of this signal. Since external fields are known to act upon MTs in neurons, the study of these fields and their interaction garners our attention.

As expected, application of a large electric field along the MT causes nearly all dipoles to orientate themselves in the direction which most closely follows that of the field. Thus, a wave of dipole flips is induced along the MT as the field is translated along the MT. This is similar to what happens as an action potential moves along an axon (figure 5). The field is felt by MTs in the vicinity of the cell membrane. Suppose the field is orientated in a direction which favours an alternate ordering for the lattice, such as is the case in MTs, these dipoles will reorientate themselves. The field acts like a pump and stores energy in the dimers. Once the field has passed, these dimers may return to their original configuration and release their stored energy. A weaker field does not actually create defects by changing the orientation of dipoles in the ground state, but may act as a bias and direct the movement of existing defects.

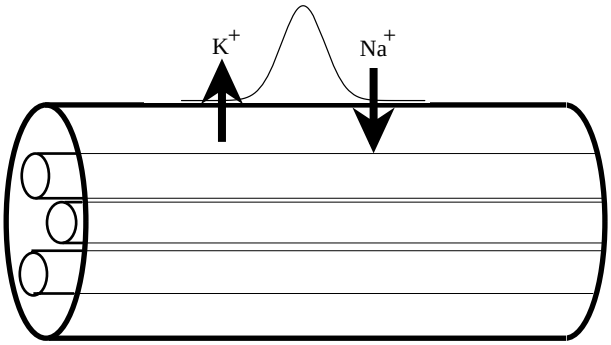

Figure 5. An action potential moving along an axon. There is an electric field caused by the potential difference and a magnetic field caused by the moving charges.

Our simulations have shown this exact behaviour. When the strength of the interacting action potential is large, such as for those MTs in close proximity to the cell membrane, a wave of structural deformation travels parallel to the action potential along the MT. As the wave reaches the MT end, its effects are unclear. Once the MT relaxes to its ground-state structure, energy should once again be available for cellular use if the structural change at the MT terminus is coupled to another cellular structure via a MAP. It might also simply serve as a cellular signal indicating when motor proteins should be activated, MT assembly instructions or any other host of functions associated with the MT terminal which could involve signalling another MT or some part of the axon terminal depending on the location of the individual MAP coupled to an MT.

Once dipole defects have been induced upon the MT lattice, they may propagate along the length of the MT. While some nonlinear effect or external guidance seems to be required, processing of these signals cannot be ruled out. In particular, signal transduction from the distal end of the axon towards the cell body is at least theoretically possible—although unlikely in our opinion. Transduction along the length of the MT is simpler to explain from the proximal end to the distal end though because of the existence of action potentials and the need to explain how a signal may be passed from one MT to another.

Our simulations place a firm limit on the minimum strength of the dipoles required for self-organization. The required dipole strength of about 320 Debye is slightly larger than the value which we estimated for tubulin (as discussed in § 2). In addition, if the angle of the dipole directions of each of tubulin's conformational states is smaller than predicted, an even larger dipole strength would be required. Should the value for tubulin be smaller than this figure, information processing must be ruled out. Energy might still be passed along due to the passage of an action potential, but it would be marked by the highly ordered configuration of the signal upon the random background. The quantity of energy associated with such an entropic change is much smaller than other values mentioned, about 0.06 kcal mol^{-1}.

On the topic of information storage in MTs, the simple introduction of thermal energy has removed the possibility of information storage in MT. The energy involved in flipping the conformation of the dimer would have to be significantly larger for

such a form of storage to be possible; not to mention the need for some kind of mechanism which would preserve the integrity of the information.

It is clear that electromagnetic properties are important in cell biology. In addition, the intrinsic polarity of MTs seems to be very important. If it were not so, one would expect the MTs within the axon to be randomly orientated. The question which might be asked is: what is the specific usefulness of a signal which is coupled to the axonal action potential and which travels along MT protofilaments inside the axon? We shall return to provide a plausible answer in the next section.

There has been additional speculation about the role of MAPs in this discussion. Certain MAPs are specific to neuronal MTs (Hirokawa 1991) and their periodic patterns of attachment are somewhat of a paradox (Dustin 1984; Hameroff 1987). Models have attempted to confirm their organizing effect; it seems that due to the interconnections and intraconnections which MAPs make between neuronal MTs, the possibility of parallel information processing is facilitated. In particular, it has been ascertained that the content of an especially important MAP, τ, increases progressively with distance to the soma (Black *et al*. 1996), indicating that its function may not only be a greater stability and assembly but perhaps enhancement of signal transfer properties. We have not pursued this sort of examination to this point; however, if even the most elementary features of MT cellular automata are experimentally corroborated, the importance of electric properties within cells will be clearly demonstrated.

4. Can signal transduction be piezoelectric?

A piezoelectric solid is usually defined as one which generates a voltage proportional to an applied mechanical force, either due to mechanical distortion or displacement of electric dipoles in its crystal lattice. Biological piezoelectricity has been observed directly in bone, DNA, RNA, myosin and collagen (Cope 1975). Piezoelectric materials are usually also pyroelectric, which means that an electric potential is generated by the application of a temperature gradient. Pyroelectricity has been directly observed and measured in tendon, bone and nerve cells. Athenstaedt (1974) was the first to describe microtubules as piezoelectric biopolymers. Piezoelectric properties of biological polymers have been reviewed by Fukada (1983), indicating that almost all biologically relevant macromolecules exhibit piezoelectricity. Included as an example of piezoelectricity was the mechanism of flagellar beating. The pyroelectric effect has also been listed as common among proteins.

Trying to link piezoelectricity with the properties of MTs, the natural starting point is to recall changes taking place in the tubulin dimer upon assembly. GTP bound to tubulin hydrolyses rapidly into GDP, imparting energy to the MT lattice. Furthermore, comparison studies of GTP and its non-hydrolysable analogue, guanylyl-(a,b)-methylene-diphosphonate (GMPCPP), by Hyman *et al*. (1995) indicate that hydrolysis results in an anisotropic deformation of the protein affected such that the non-hydrolysed monomer length is increased by approximately 1.5 Å with the opposite effect taking place in the perpendicular direction.

At neutral pH, the hydrolysis of GTP in solution proceeds according to the chemical reaction

$$\mathrm{GTP}^{4-} + \mathrm{H_20} \rightarrow \mathrm{GDP}^{3-} + \mathrm{HPO}_4^{2-} + \mathrm{H}^{+} + \Delta E, \tag{4.1}$$

where $\Delta E = 8.7\,\mathrm{kcal\,mol^{-1}}$. It is also worth pointing out that the release of a proton in this reaction may play an important role in both dielectric and conductive properties of the cytoplasm.

It appears that the amount of hydrolysis energy changes drastically when GTP is bound to either a single tubulin or a whole microtubule. This was studied by Caplow *et al*. (1994) using GMPCPP, which stabilizes microtubules. In solution, the hydrolysis of GMPCPP releases $5.18\,\mathrm{kcal\,mol^{-1}}$, which is reduced to $3.79\,\mathrm{kcal\,mol^{-1}}$ for GMPCPP attached to a tubulin dimer and to only $0.90\,\mathrm{kcal\,mol^{-1}}$ when GMPCPP is embedded in a microtubule structure. The difference in these numbers is believed to indicate the amount of energy stored in the microtubule structure. However, the last figure also indicates that upon assembly an excess of energy is imparted to the tubulin subunits without an apparent designation. It has been suggested that this excess amount of energy could be used to change protein bond strengths, or cause conformational changes of tubulin, or even be stored as fault energy of the lattice which may be released later through a collapse catastrophe. This energy can conceivably be harnessed in the form of mechanical work, for example, by coupling disassembly to the vesicle or chromosome movement or even providing the coordinated behaviour of the ciliary motor proteins.

Several groups of researchers have developed nonlinear models of energy propagation along a microtubular protofilament. Chou *et al*. (1994) showed that kinks and pulses excited by the energy freed in the GTP hydrolysis can propagate along MTs due to elastic coupling between tubulin dimers. Another model of solitary wave formation was proposed by Sataric *et al*. (1993) and further developed by Trpišova & Tuszyński (1997). The working assumption here is that tubulin dimers possess dipole moments which are spontaneously ordered at physiological temperature. Consequently, solitary waves carrying the free portion of the hydrolysis energy correspond to kink-type domain walls connecting two regions of the protofilament with opposite electric polarizations.

The physical model is based on the lattice Hamiltonian

$$H = \sum_{n=1}^{N}\left[\tfrac{1}{2}M\left(\frac{\mathrm{d}u_n}{\mathrm{d}t}\right)^2 + \tfrac{1}{2}K(u_{n+1}-u_n)^2 - (\tfrac{1}{2}\alpha_2 u_n^2 - \tfrac{1}{4}\alpha_4 u_n^4) - cu_n\right], \qquad (4.2)$$

where u_n represents the projection on the protofilament axis of the dimer's conformational change (coupled to the dipole moment) and the various other terms represent the kinetic energy, the elastic restoring energy and the effective nonlinear potential, while the last term is responsible for the effect of external (electric or pressure) fields on the system of coupled dipoles placed on tubulin molecules, each of mass M.

Furthermore, cellular MTs are embedded in cytosol, which is a liquid ion-filled solution which interacts with the MTs both via electric forces and by providing a viscous medium which damps the motion of tubulin dimers. This latter effect can be modelled by including a frictional force $F_{\mathrm{v}} = -\gamma\partial u_n/\partial t$ in the equation of motion. Taking the continuum limit such that $u_n(t) \to u(x,t)$ yields the following equation of motion for the displacement variable:

$$M\frac{\partial^2 u(x,t)}{\partial t^2} - KR_0^2\frac{\partial^2 u}{\partial x^2} - \alpha_2 u + \alpha_4 u^3 + \gamma\frac{\partial u}{\partial t} - q_{\mathrm{eff}}E = 0. \qquad (4.3)$$

Somewhat surprisingly, an analytic kink-type solution has been found in the form

$$u(\xi) = u_2 + \frac{u_1 - u_2}{1 + \exp[(u_1 - u_2)\xi/\sqrt{2}]}, \tag{4.4}$$

where u_1 and u_2 are the real roots of the cubic polynomial in equation (4.3) and ξ is the moving coordinate $\xi = x - vt$. The sound velocity of MTs was estimated elsewhere as $v = 610\,\mathrm{m\,s^{-1}}$ (Sirenko *et al.* 1996). The damping coefficient γ was estimated to be $\gamma = 5.2 \times 10^{-11}\,\mathrm{kg\,s^{-1}}$ (Trpišova & Tuszyński 1997). Consequently, it was determined that for sufficiently small electric fields E, the velocity of kink propagation, v, is proportional to the electric field strength E and it ranges from $10^{-2}\,\mathrm{m\,s^{-1}}$ for $E \sim 2\times10^5\,\mathrm{V\,m^{-1}}$ to $10^{-4}\,\mathrm{m\,s^{-1}}$ for $E \sim 10^2\,\mathrm{V\,m^{-1}}$. These numbers appear to be on the high side of the known MT-associated processes (assembly, disassembly speeds or motor protein velocities) but one should also be aware of the great sensitivity of v to the dielectric constant of the medium and to the presence of impurity potentials along the path of a moving kink which was studied numerically. In fact, for large enough potential wells or bumps, kink motion can be stopped altogether (Trpišova & Tuszyński 1997). The question arises as to what happens to the energy transported by a kink excitation. We may speculate that it is transferred to another MT via an attached MAP or that it could play an important role in the movement of a motor protein. Another possibility is that it creates a domain wall between two portions of a MT protofilament in which tubulin dimers are in different dipolar and conformational states. This could be an important factor in developing microscopic models of dynamic instability.

Models have also been developed which explicitly account for the coupling between tubulin dipoles and the conformational (elastic) degrees of freedom (Trpišova & Tuszyński 1997). A phenomenological Landau–Ginzburg free-energy expansion has been formulated for the entire stable MT in terms of the total dielectric polarization P and the mechanical stress σ which is coupled to P via the piezoelectric effect. The free energy then takes the form

$$F = F_0 + \tfrac{1}{2}AP^2 - \tfrac{1}{4}BP^4 + \tfrac{1}{6}CP^6 - \tfrac{1}{2}e\sigma P^2 + \tfrac{1}{2}D(\partial P/\partial x)^2 - \tfrac{1}{2}s_0\sigma^2. \tag{4.5}$$

The time-evolution of the order parameter (net polarization P) is given by the time-dependent Landau–Ginzburg equation

$$\frac{\partial P}{\partial t} = -\Gamma\frac{\delta F}{\delta P}, \tag{4.6}$$

where Γ is the phenomenological Landau–Khalatnikov damping coefficient providing a time-scale for relaxation processes. In our case this equation takes the form

$$\frac{\partial P}{\partial t} = \Gamma(AP - BP^3 + CP^5 - e\sigma P) + \Gamma D\frac{\partial^2 P}{\partial x^2}, \tag{4.7}$$

and it is coupled to the stress–stain relationship

$$\epsilon = \frac{\partial u}{\partial x} = -\frac{\partial F}{\partial \sigma} = \tfrac{1}{2}eP^2 + s_0\sigma. \tag{4.8}$$

These two equations can be effectively decoupled by taking note of the fact that ϵ also satisfies the wave equation

$$\rho\frac{\partial^2 \epsilon}{\partial t^2} = \frac{\partial^2 \sigma}{\partial x^2}, \tag{4.9}$$

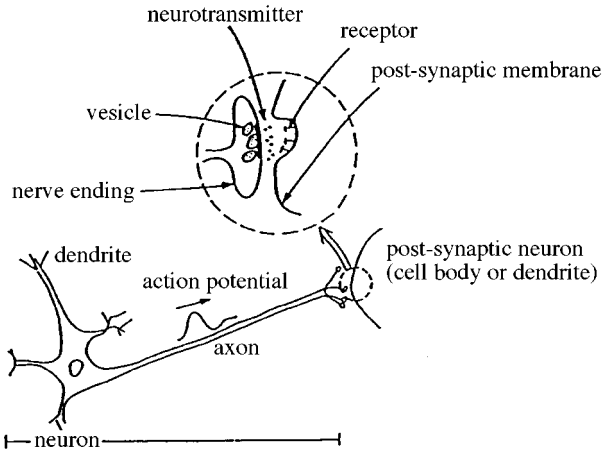

Figure 6. Schematic diagram of a neuron. Inset shows a neuron–neuron synapse.

which results in an effective equation for travelling polarization waves:

$$\Gamma D\frac{\mathrm{d}^2P}{\mathrm{d}\xi^2}+v\frac{\mathrm{d}P}{\mathrm{d}\xi}-\Gamma(AP-\tilde{B}P^3+CP^5)=0, \tag{4.10}$$

where $\xi = x - vt$ and $\tilde{B}$ is a 'dressed' expansion coefficient. This model was also studied numerically (Trpišova & Tuszyński 1997). The polarization wave describes a localized nucleation which moves with a constant velocity along a protofilament. Above the transition temperature for the paraelectric phase to the ferroelectric phase transition, which could be in the physiological range for most of electric field values, collisions of coupled $P-\sigma$ waves with an impurity potential result in the formation of a constant stress along the MT. This could lead to a build-up of fault energy and a subsequent disassembly. This model has also been analysed in the presence of an external pressure applied to a MT. Several effects have been seen in these latter simulations: (a) a decrease in the kink's propagation velocity down to the $\mu\mathrm{m\ s}^{-1}$ range when hydrostatic pressures are applied; (b) a dielectric phase transition which may be induced by applying pressure to the microtubule. Some numerical estimates were made and compared to the observed values of Young's modulus, Y, in the protofilament direction where $Y = 0.5\times10^9\ \mathrm{N\ m}^{-2}$ has been reported (Mickey & Howard 1995). Our estimate of the longitudinal stresses which accompany the propagation of a kink along the protofilament is $\sigma = 10^6\ \mathrm{N\ m}^{-2}$.

We conclude that nonlinear models of energy transfer along microtubules provide a conceptual link between the excess energy released in GTP hydrolysis directly after tubulin assembly and the various processes associated with the functions of MTs, especially motor protein motion, chromosome segregation forces and disassembly velocities.

In the context of neuronal MT functioning, the piezoelectric properties of MTs may offer a very attractive connection between the internal structure of the axon and its function, namely synaptic communication (see figure 6). The first link that may be established has to do with the control mechanism of exocytosis of neurotransmitters. Segel & Parnas (1991) argued convincingly that the Ca^{2+} wave in the extracellular medium is insufficient to explain quantitatively the sensitivity of the neurotransmitter release mechanism to depolarization at the release site. They pro-

posed the existence of an additional polarization mechanism which, in our opinion, may well be the coupled polarization–stress wave propagating along the MT that accompanies the action potential motion.

The other possible link involves the architecture of neurons which number 10^{10} in the brain and, through sensory stimulation, each of them develops an extensive dendrite tree with a signal target made up of 10^3–10^5 other neurons. These nearest-neighbour neurons are connected via synapses mentioned above. In some neurons over 99% of their surface area is accounted for in the dendritic tree. The functioning of the dendritic trees consumes up to 60% of the brain's energy (Mel 1994). How can individual synaptic connections within such a tree be maintained or abandoned depending on their usefulness or lack thereof, respectively? As argued earlier, when the action potential travels along the axon it affects the MTs dipoles such that the GTP energy that MTs constantly receive from the cell is smoothly transferred from one MT end to the other. We found that the propagation of dipole kinks is feasible even at velocities in the 1–20 $\mathrm{m\,s^{-1}}$ range, roughly corresponding to the action potential velocity of propagation. We also stressed here that there is electroconformational coupling in MTs. That means that stable MTs have straight protofilaments (tense). However, unstable MTs have protofilaments which curve away from the axis (relaxed). Instability comes about when too much energy is delivered to MTs and it is stored in them without an outlet. For example, it can get stored in the form of mechanical fault energy, causing crystal lattice defects. Therefore, when action potential signals are very infrequent, MTs may have difficulty getting rid of excess energy, so they become curved or full of defects. This would eventually lead to several possible modes of MT degeneration: (a) falling apart of the middle part if, for example, MAPs are also weakened. This could be the case with Alzheimer's disease where τ protein does not clamp onto the scaffold structure of MT bundles. The consequence would be that axons themselves would be affected and synaptic connections destroyed. (b) If they don't fall apart, they may still experience negative effects due to piezoelectricity. The MTs would, for example, build unidirectional stress that could curve their axis away from the straight line of the synaptic connection. The result could be the two ends on the opposite sides of the synapse moving away from each other. They may eventually find other new partners with which to pair up within the dendritic tree. The latter possibility would explain why synaptic connections are eliminated if they are not used sufficiently.

5. Can MTs conduct electrical currents?

Conjectures regarding the possibility of electrical conduction in biological polymers were originated by Szent-Györgyi in the 1940s and elaborated on later by Pullman & Pullman (1962) who pointed to the role of delocalized π-electrons in biochemical compounds. They predicted the existence of both extrinsic and intrinsic semiconducting properties of protein polymers. Pethig (1982) performed band-structure calculations for some simple protein polymers and found the band gap to be of the order of 6.0 eV with a band width of approximately 1.5 eV, indicating that they would most likely be insulators unless disorder in the structure was introduced to drastically reduce the energy gap.

Table 1. *Potential functions of molecular complexes as bioelectronic materials*

function	molecular complexes
wiring	polyene antibiotics conductive polymers
storage	bacteriorhodopsin reaction centres (PS II) cytochromes blue proteins ferritin collagen, DNA
gates and switches	bacteriorhodopsin photosynthetic systems cell receptors ATPase
input/output devices	photosensitive proteins enzymes receptors metal–protein complexes

Table 2. *Abundance of n-type and p-type amino acids in α- and β-tubulin*

amino acid	electronic type	% in α-tu	% in β-tu
Asp	*n*	10.3	11.1
Lys	*p*	3.9	3.8

A general discussion regarding the potential for bioelectronic devices based on molecular complexes predicts a range of fascinating possibilities, as shown in table 1 following Tsong (1989) and Wangermann (1980).

Based on table 1, one might expect MTs under suitable conditions to provide wiring for the transmission of electrical pulses (e.g. inside axons or as mitotic spindle apparatus) or perform input/output functions using electromagnetic signals if they can be photosensitive under special circumstances (as is believed to be the case in centrioles and in the phototaxis mechanism of cilia). A recent paper (Insinna *et al*. 1996) has given an exhaustive account of the accumulated evidence for the participation of MTs in electrical conduction within the cell via electron or proton transfer mechanisms which can be coupled with GTP hydrolysis. In fact, Koruga & Simić-Krstic (1990) pointed out that semiconducting properties of MTs are to be expected simply on the basis of the tubulin's constitution from the linear *n*-type (Asp) or *p*-type (Lys) amino acids. This is shown in table 2 and would indicate that there is approximately three times more *n*-type than *p*-type amino acids based on the number of amino acid residues and, hence, one expects an excess of mobile electrons to exist.

Using the above premise we have undertaken to examine the issue of conductivity in a theoretical detail. For comparison purposes, we assumed the presence of just

two conduction electrons for each tubulin dimer, leading to the conduction electron density of $n_0 = 10^{19}$ cm^{-3}. This may be an overestimation, since in comparison with other materials, this value is higher than typical semiconductor concentrations, usually 10^{13}–10^{17} cm^{-3}, but is much less than typical metals which have a conduction electron density of 10^{22}–10^{23} cm^{-3}. However, the electrons are expected to have relatively low mobilities unless they are excited from the ground-state configuration. The excitation energy is a function of both the number of electrons within the protofilament and its size. Suppose that the mobility of excited electrons is at least similar to the mobility of electrons within semiconductors such as Si, where the electron mobility, μ_e, is about 1300 cm^2 V^{-1} s^{-1}. The conductivity, σ, is given in a semiclassical model by

$$\sigma = ne\mu_e, \tag{5.1}$$

where n is the conduction electron density and e is the electron charge. The electron density is given as

$$n = n_0 e^{-\Delta/kT}, \tag{5.2}$$

where n_0 represents the total number of electrons per cm^3. If we assume that the gap between valence and conduction bands, Δ, is about eV, which is the small barrier height in our model, then at physiological temperature, some of the carriers will be thermally excited and should be available to conduct. Applying equation (5.1), a conductivity of about 10^{-2} is expected for the protofilament:

$$\sigma \sim (10^{25} e^{-0.40/0.026})(1.6 \times 10^{-19})(0.13) \sim 0.04\,\Omega^{-1}\,\mathrm{m}^{-1}. \tag{5.3}$$

However, if the hybridization of electronic orbitals lowers the gap to a value closer to zero, the expected conductivity would be significantly higher:

$$\sigma \sim (10^{25})(1.6 \times 10^{-19})(0.13) \sim 2 \times 10^5\,\Omega^{-1}\,\mathrm{m}^{-1}. \tag{5.4}$$

This is an upper limit on conduction in MTs due to the optimistic choice of electron mobility. This value should be compared to values in excess of 10^8 for copper and other good conductors, 10^7 for lesser conductors and semimetals. Typical semiconductors such as Si and Ge have intrinsic conductivities of 10^{-3} to 10^{+1} at room temperature, but when heavily doped the conductivity may rise to between 10^4 and 10^5.

In subsequent quantum-mechanical calculations each protofilament is pictured as a chain of periodically distributed potential double wells whose two sites represent two binding sites, one each on each monomer between which the electron may hop (figure 7). We can estimate the relevant parameters of the well depth and the well width from kinetic studies and with a knowledge of the molecule's overall geometry. Once the bound states and their energies are known for this system, this knowledge may be applied to a second-quantization scheme. Hopping along the protofilament by electrons presumably has an energy comparable to the binding energy. We have estimated 0.4 eV for intradimer hopping. Thus, a single hydrolysis event is not expected to cause disassembly.

The results for the single-electron eigenstates of a double quantum well may be found in a rather straightforward manner using a transfer matrix method for the eigenfunctions of the time-independent one-dimensional Schrödinger equation:

$$\hat{H}\psi = \frac{\hat{p}^2}{2m}\psi + \hat{V}\psi = E\psi. \tag{5.5}$$

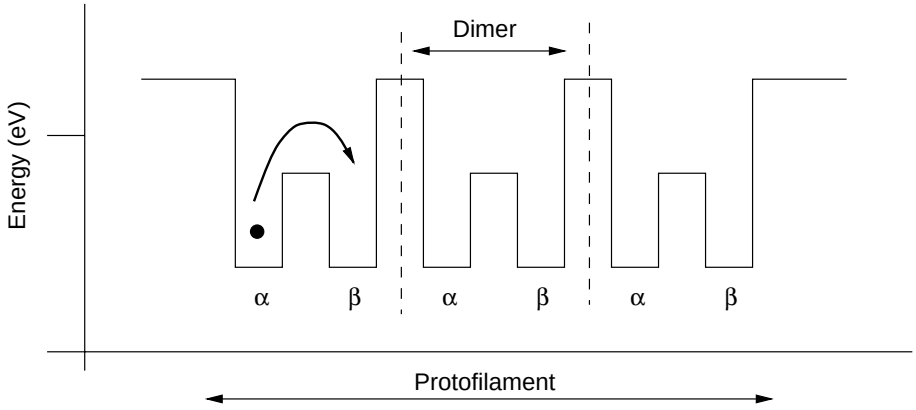

Figure 7. Model of the MT protofilament with a binding site located on each α-monomer and β-monomer.

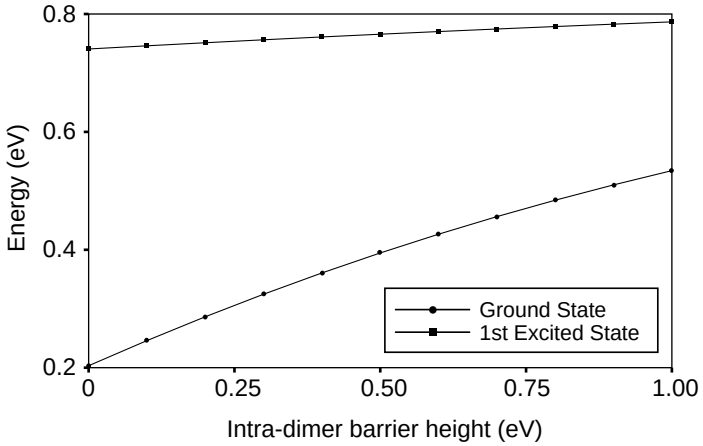

Figure 8. Variation of the bound-state energies of a dimer with the central barrier height.

In figure 8 we show the results of our numerical solutions for the two bound states of a single dimer (ground and excited) as a function of the energy of the central potential barrier. One may then calculate the energy of such states for a sequence of n such dimers. This leads to the development of bands as hybrid orbitals stretch across the polymer. Roughly speaking, one band is of hybridized symmetric orbitals and the high-lying band of hybridized antisymmetric orbitals (figure 9). The separation of the two bands and the spread of each individual band is important. They determine the values of the parameters which shall be used in the tight-binding Hubbard model which shall be used to model the polymer. The Hubbard model is the simplest second-quantized model to capture all of the essential features of a real system of interacting particles (Lieb 1995). In this model, the particles, i.e. electrons, are fundamental excitations described by the Hamiltonian

$$\hat{H} = \sum_{i,\sigma} \epsilon_i \hat{C}^{\dagger}_{i\sigma} \hat{C}_{i\sigma} + \sum_{i \neq j,\sigma} t_{ij} \hat{C}^{\dagger}_{i\sigma} \hat{C}_{j\sigma} + \sum_{i} U_i \hat{C}^{\dagger}_{i\uparrow} \hat{C}_{i\uparrow} \hat{C}^{\dagger}_{i\downarrow} \hat{C}_{i\downarrow}, \tag{5.6}$$

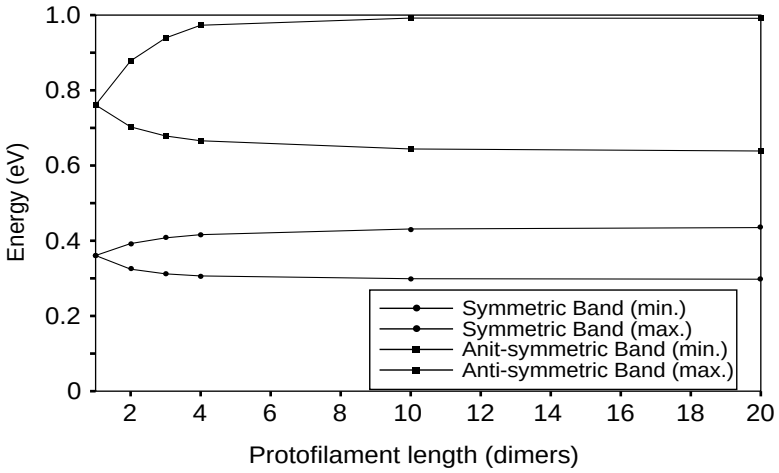

Figure 9. Band formation as the protofilament is lengthened.

where the operators $\hat{C}^{\dagger}_{i\sigma}$ and $\hat{C}_{i\sigma}$ are the usual fermion creation and annihilation operators, and where $i = 1, \ldots, 2n$ represent the two sites on each of the n dimers. The ϵ_i represent the potential energy at each site and the kinetic terms t_{ij} account for hopping from one site to another. We are accounting for nearest-neighbour interactions in the model, but there are two different kinds of interactions depending on whether an electron hops within a dimer, or between dimers. Hence, this kinetic parameter has two different values along the chain: t_{d} or t_{l}, respectively. The final term accounts for electron–electron repulsion now that we have gone to a many-electron system. In our simple model, this is limited to an on-site interaction. To this point, we have made each of the site energies equivalent ($\epsilon_i = \epsilon$); since the Hamiltonian conserves the particle number, this term may be ignored as a trivial constant. We have also made the electron repulsion the same at all sites ($U_i = U$). We expect $U = 2.0\,\mathrm{eV}$, which is the energy associated with two bare electrons lying about 0.7 nm apart. This choice seems reasonable within a well of width 2.0 nm.

On comparison with figure 9, which shows the band formation in the quantum well formulation, we can assign values to t_{d} and t_{l}. The two bands are separated by about 0.40 eV, so $t_{\mathrm{d}} \approx 0.20\,\mathrm{eV}$ and using the bottom band to estimate t_{l}, it widens until it is about 0.10 eV thick, so $t_{\mathrm{l}} \approx 0.05\,\mathrm{eV}$.

Suppose an external field is applied; we want the conductivity that is the response to the total electric field in the solid. This conductivity takes into account all of the currents induced by the external fields which create their own fields. In other words, we are looking for the self-consistent conductivity:

$$J_\alpha(r,t) = \sum_\beta \sigma_{\alpha\beta}(q,\omega) E_\beta \mathrm{e}^{\mathrm{i}qr - \mathrm{i}\omega t}. \tag{5.7}$$

This tensor, $\sigma_{\alpha\beta}$, is the conductivity we are looking for which relates the macroscopic electric field to the currents of the system which may be measured.

In terms of the Hamiltonian's eigenstates $|n\rangle$ and frequency dependence, conduc-

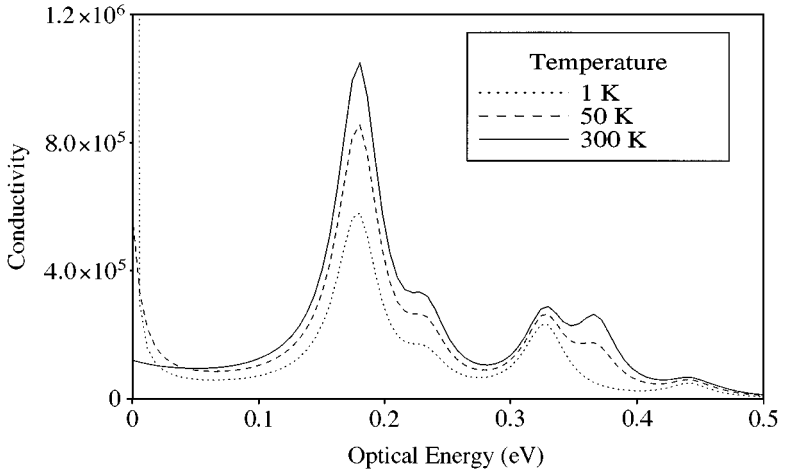

Figure 10. Conductivity is plotted as a function of the optical energy for a short protofilament. The spectrum changes as the temperature is raised. Note the single peak which becomes a double peak close to 0.35 eV.

tivity is expressed as (Mahan 1981)

$$\sigma(\omega) = \frac{\pi}{Z}\frac{1}{\omega}\sum_{m,n}(\mathrm{e}^{-\beta E_m} - \mathrm{e}^{-\beta E_n})|\langle n|j_\alpha|m\rangle|^2\delta(\omega - (E_n - E_m)). \tag{5.8}$$

Modelling the protofilament as a Hubbard chain, the eigenstates are found by exact diagonalization techniques and these are then used as input for the Kubo model of electrical conduction. The δ-functions of the last expression are replaced with Lorentzians of finite width as follows:

$$\delta(\omega - a) \to \frac{1}{\pi}\frac{\epsilon}{(\omega - a)^2 + \epsilon^2}. \tag{5.9}$$

This approximates relaxation processes and the degree of experimental precision. In addition, the temperature which we have chosen, 300 K, is approximately physiological temperature since conductivity is temperature dependent. In the Hubbard chain model of the MT protofilament at 0 K, there is conduction only at the frequencies which are equal to jumps between the ground state and each of the excited states. As the temperature is raised, the excited states may themselves be populated. Consequently, more peaks are observed as transitions between excited states may also contribute to the overall conduction (figure 10). Now, we are interested not only in the peak values of conductivity and how it may vary with the protofilament length, but particularly also in how the conductivity varies with the number of charge carriers. The tubulin which forms protofilaments is composed of two dimers, α and β. Each of these monomers has several isotypes. MTs localized in different places within the body differ in their isotypic composition. The isotypic composition may also change in a given location as a function of the cell cycle (Moskowitz & Oblinger 1995). These isotypes of α- and β-tubulin have different regulatory roles and differ almost superficially along certain side chains. That is, these changes do not seem to affect the MT structure, or cause the assembly properties to change much, but may be of utmost importance to the conducting properties of MTs by introducing electron or hole doping into this picture. For example, distinguishable β-tubulin

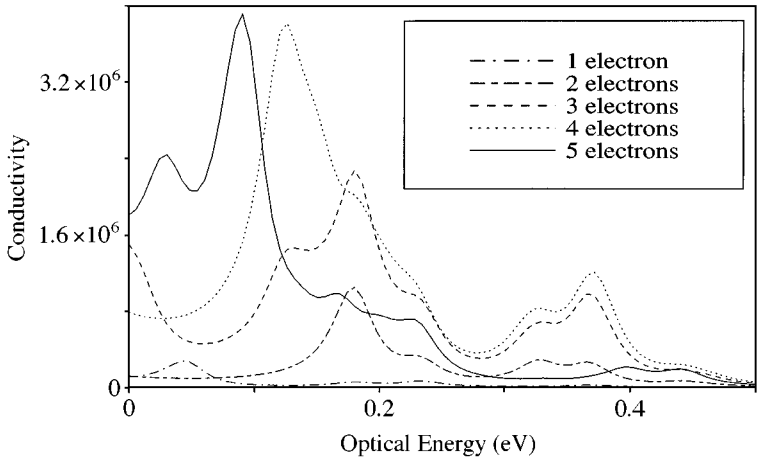

Figure 11. Conductivity is plotted as a function of the carrier concentration.

isotypes have been found to be differentially distributed among the peripheral and central axoplasm. In addition to the interactions these specific isotypes may have with MAPs, certain amino acid residues on these side chains may be hydrolysed or glutamylated to varying extents and this modification may provide additional (or fewer) charge carriers. Consequently, we hope to find the best carrier concentration for conduction which might dictate a specific ratio between the levels of the various tubulin isotypes which should be incorporated into MTs.

Typical MTs in which we are interested span 1000 or more subunits. Such objects which are of the order of a few microns long could be experimentally studied. However, these cannot be tackled theoretically using the present techniques because of computational limitations related to the diagonalization and multiplication of large matrices. As a result, the work is being carried out on short filaments of a few dimers length.

Figure 11 displays a sample of conductivity curves in a protofilament of three dimers with various numbers of electrons. The single-electron case is expected to differ from the others since there is obviously no Coulomb repulsion in such a system and it turns out to have the lowest conductivity. Conductivity seems to increase as electrons are added to the system until it is precisely half full. The situation at half-filling is somewhat of a puzzle but we surmise that the low conduction is the result of more localized electrons at that specific fractional filling. One electron may be confined to each monomer and Coulomb repulsion avoided. However, the movement of any electron ruins this energetically stable state. At other fractional fillings, electron movement is possible without disturbing the energy of the system similarly.

Now, while our results are preliminary to this point, it is interesting to attempt to make predictions for the entire MT. This involves extending the Hubbard model to a second dimension. Hopping is allowed in a second direction about the helix in addition to along the protofilament. This adds several complications; first, there are many more states in a model of this system. Consequently, the matrix which must be diagonalized is much larger. As the density of states is much greater in the MT, one may expect that the conductivity will also be higher—that is in an MT of the

same length as a protofilament. Physically, one might rationalize this simply. There are a larger number of paths available for the electron to move from one end to the other; consequently, one would expect the resistivity to be lower—conductivity, which is the inverse of the resistivity would therefore be larger. In addition, the close spacing of energy levels implies that there should be more peaks at lower energies corresponding to the level spacing. Consequently, conduction along the MT should be greatly improved over protofilament conduction, especially at lower frequencies. The added complication is that conductivity becomes a tensor with the introduction of the additional protofilaments in the MT. In axonal MTs the field is expected to be radial while it would be conduction along the MT which is of interest.

There are also questions of conductivity if the charge carriers are not electrons but hydrogen ions (H^+). Proton hopping may be modelled in a similar way but protons have a much larger mass than do electrons. The higher mass means that energy levels are more closely spaced; again this probably means higher conduction at lower frequencies, but for our choice of parameters for the double quantum well, no bound states exist. Thus, binding of the protons must be somewhat larger. This would therefore have a negative effect on the conductivity. No meaningful statement can be made on protonic versus electronic conduction without further investigation.

6. Can MTs function as quantum computers?

It is a very attractive proposition to consider protein assemblies performing the task of a computer. Protein-based computers could operate 10^3 times faster than semiconductor-based computers. Furthermore, they could be designed one atom at a time, offer parallel processing architecture, three-dimensional data storage and a number of other features. In fact, a case has recently been made (Bray 1995) to view the already existing intracellular assemblies of proteins as computational elements which in essence constitute the cell's equivalent of a nervous system. Many aspects of cell behaviour display capacity for information processing independent of the genome and are controlled by proteins, e.g. motility. Bray (1995) maintains that GTP supply is the key element as it activates proteins while GDP deactivates them, which is consistent with our earlier discussions. Protein circuits in cells include hundreds of different channels, receptors and kinases which together monitor and respond to internal and external environmental stimuli. Can MTs be viewed as part of such circuitry? If so, how can their functioning as information processors be accomplished?

Some evidence links the cytoskeleton with information processing and cognitive function. Production of tubulin, the MT subunit and MT activities is correlated with peak learning, memory and experience in baby chick brains. When baby rats begin their critical learning phase for the visual system (when they first open their eyes), neurons in the visual cortex begin producing vast quantities of tubulin (Cronly-Dillon 1974). Tubulin production is drastically reduced when the critical learning phase is over (when the rats are 35 days old). Bensimon & Chernat (1991) found that selective destruction of brain MTs by the drug colchicine caused cognitive defects in learning and memory which mimic the clinical symptoms of Alzheimer's disease, in which the cytoskeleton becomes entangled. Further suggestion for cytoskeleton computation and/or information storage stems from the spatial distribution of discrete sites (or states) in the cytoskeleton. For example, tubulin subunits in closely arrayed MTs have a density of about $10^{17}\,\mathrm{cm}^{-3}$, which is very close to the theoretical limit for

Table 3. *Characteristic physical quantities describing MTs and their environment.*

tubulin dimer mass	110 kDa $\simeq 10^{-21}$ kg
dielectric constant	5–10
mobile charge	1–2e^- $\simeq 10^{-19}$ C
electric field strengths	
in membrane	10^7 V m^{-1}
in cytoplasm	10^{-1}–10^1 V m^{-1}
temperature	300 K
velocity	
phonon	600 m s^{-1}
tubulin in cytoplasm	1 μm min^{-1}
charge in axon	1–2 m s^{-1}
motor protein	0.5–2 μm s^{-1}
light wavelength (λ)	400–700 nm

charge separation (Gutmann 1986). Thus the cytoskeleton polymers have maximal density for information representation by charge, and the capacity for dynamically coupling that information to mechanical energy and chemical events via cooperative dipole states.

Recently, Hameroff & Penrose (1996) advanced the hypothesis which in a nutshell states that MTs are biological quantum computers providing a molecular substrate for the emergence of consciousness. In their model, called orchestrated objective reduction, or Orch OR for short, MTs' tubulin dimers are viewed as existing in a quantum superposition state which may self-collapse (hence the term objective reduction) upon reaching a quantum gravity threshold. The resultant wavefunction collapse event was linked by these authors (Hameroff & Penrose 1996) with numerous synaptic/neural functions and, in particular, with the formation of a thought process. While the Orch OR hypothesis cannot be proved or disproved at present, we will try to assess its validity within the context of the physical properties of MTs presented earlier in the paper.

In this connection, it is worthwhile recalling several thoughts on the topic of physics, computation and biology verbalized not too long ago by Hopfield (1991). First, he stated that: 'the human brain is the most mysterious and complex of these biological computational systems'—which would perhaps give legitimacy to searches for very exotic explanations of its functioning. However, he also said that 'contrary to the expectations of a long history of ill-prepared physicists approaching biology, there is absolutely no indication that quantum mechanics plays a significant role in biology'. He emphasized the role of complexity in biological systems where a change in a meaningful bit of information will have an effect on macroscopic behaviour of a living system. This is not so in physical systems.

Returning now to the issue of MTs, we wish to summarize the key physical parameters describing these protein polymers and their cellular environment (cytosol). These are shown in table 3. Based on these numbers and our earlier discussions throughout this paper we can put together a summary of energy-scale estimates for the processes that have been either observed or postulated to play a role in the functioning of MTs. This is summarized in table 4. For better clarity, this information is illustrated graphically in figure 12. What are the general conclusions we can draw regarding these processes? First of all, for all intents and puposes, gravitational effects

Table 4. *Estimates of energy scales*

chemical (hydrolysis)	
free GTP	0.2 eV
Tu-GTP	0.12 eV
MT-GTP	0.03 eV
electrical (qE)	10^{-4}–10^{+1} eV
dipole–dipole ($d^2/\epsilon r^3$)	10^{-2}–10^{-1} eV
thermal (kT)	*ca.* 0.02 eV
phonon ($\hbar\omega$)	*ca.* 10^{-4} eV
$\omega = \sqrt{K/M}$	
light (hc/λ)	*ca.* 1–2 eV
kinetic ($mv^2/2$)	
motor protein	3×10^{-15} eV
electron	*ca.* 10^{-10} eV
gravitational ($GM_{\mathrm{Tu}}^2/r_{\mathrm{Tu}}$)	10^{-27} eV
mechanical conformation ($kx^2/2$)	
$E_{\parallel}$	0.3 eV
$E_{\perp}$	0.03 eV

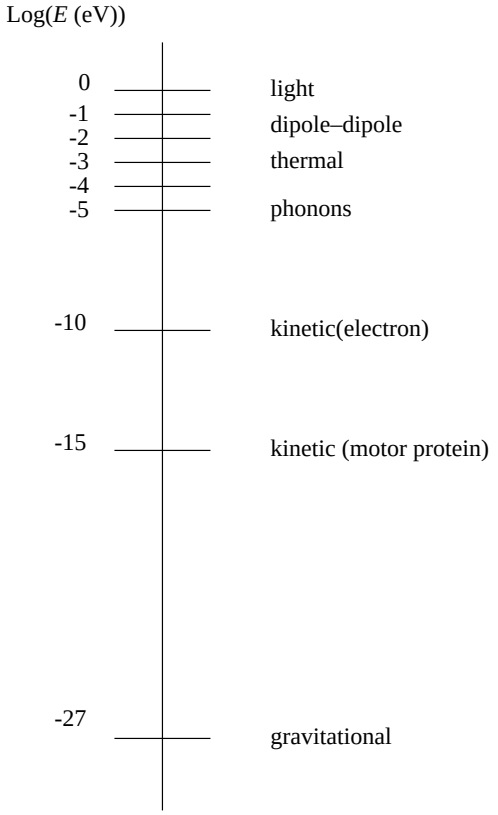

Figure 12. Graphical display of relative energies of MT-associated processes.

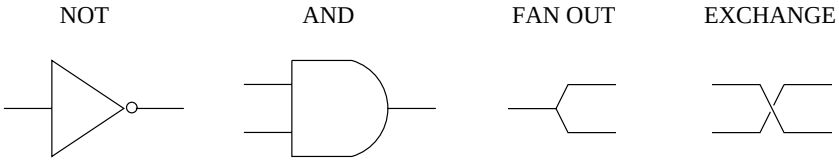

Figure 13. Basic function elements for a quantum computer.

should be entirely overshadowed by the remaining processes. Secondly, it is likely that electrons and motor proteins are guided by electric fields in order to overcome thermal noise. There is also substantial scope for cross-effects between different types of interactions, e.g. (a) photoconduction; (b) mechano-chemical coupling; (c) chemically triggered dipole reversals; (d) electromechanical; and (e) a possible induction of magnetic fields by electric currents. Turning now specifically to the Orch OR model of Hameroff & Penrose (1996), the chief difficulties of reconciling their proposal with our analysis can be listed as follows.

(i) The size of the tubulin protein is probably too large to make quantum effects easily sustainable.

(ii) Conformational effects are expected to involve distances *ca.* 10Å, which, again, are larger than those called for in the Orch OR model.

(iii) Physiological (room) temperature requirements make it extremely difficult to defend the use of the quantum regime due to the persistence of thermal noise.

(iv) A possible effect mediating against thermal fluctuations might be some form of screening of tubulin from the cell's 'noisy' environment. As discussed earlier, MTs are extremely sensitive to their environment, especially ionic and microelement concentrations. Hence, we doubt that MTs can be shielded from their environment.

(v) It appears that the two (or possibly more) conformational states of tubulin are separated by a sizeable potential barrier which again requires an external stimulus (such as GTP hydrolysis) to overcome it.

(vi) The calculations of the 500 ms preconscious processing time may be directly related to the action potential's travel time along the axon plus the refractory lag time in synaptic transmission, rather than to the quantum collapse time.

We, therefore, believe that the Orch OR model is not tenable for MT functioning. Is there still another possibility, that MTs are quantum computational devices? Feynmann (1986) presented a very lucid analysis of a quantum-mechanical computer which basically deals with a physical system composed of two-state units. The four key operations are shown in figure 13. Feynmann translated the action of these logical elements into the language of second quantization and found corresponding Hamiltonian terms. Recently, an application of these concepts to a system of quantum dots was made (Brum & Hawrylak 1997) and it was demonstrated that a quantum exclusive-OR gate can be made. The Hamiltonian relevant in this case was of the Hubbard type and it represents the same class of problems as the electronic conduction model in a MT presented in § 5. The full set of quantum functions shown in figure 13 can be realized through the coupling provided by MAPs with the proviso that there exists a mechanism maintaining the two-level structure of mobile electronic states.

This research has been supported by an NSERC grant awarded to J.A.T. and by an NSERC post-graduate fellowship awarded to J.A.B.

References

Amos, L. 1995 *Trends Cell Biol.* **5**, 48.

Athenstaedt, H. 1974 *Ann. N.Y. Acad. Sci.* **238**, 68.

Audenaert, R., Heremans, L., Hevemans, K. & Engelborghs, Y. 1989 *Biochim. Biophys. Acta* **996**, 110.

Baas, P. & Black, M. 1990 *J. Cell. Biol.* **111**, 495.

Baas, P., Deitch, J., Black, M. & Banker, G. 1988 *Proc. Natn. Acad. Sci. USA* **85**, 8335.

Barthou, H., Brière, C., Caumont, C., Petitprez, M., Kallerhoff, J., Borin, C., Sonvre, A. & Alibert, A. 1997 *Plant Cell. Rep.* **16**, 310.

Bayley, P., Schilstra, M. & Martin, S. 1990 *J. Cell Sci.* **95**, 33.

Bensimon, G. & Chernat, R. 1991 *Pharmacol. Biochem. Behav.* **38**, 141.

Berg, H. 1995 *Bioelectrochem. Bioenerg.* **38**, 153.

Binder, K. 1988 *Monte Carlo simulation in statistical physics: an introduction.* New York: Springer.

Black, M. M., Slaughter, T., Moshiach, S., Obrocka, M. & Fisher, I. 1996 *J. Neurosci.* **16**, 3601.

Bray, D. 1995 *Nature* **376**, 307.

Brown, J. A. & Tuszyński, J. A. 1997 *Phys. Rev.* E **56**, 5834.

Brum, J. A. & Hawrylak, P. 1997 *Superlattices Microstruct.* **22**, 1.

Caplow, M., Ruhlen, R. L. & Shanks, J. 1994 *J. Cell. Biol.* **127**, 779.

Chou, K. C., Zhang, C. T. & Maggiora, G. M. 1994 *Biopolymers* **34**, 143.

Chrétien, D. & Wade, R. 1991 *Biol. Cell* **71**, 161.

Chrétien, D., Fuller, S. & Karsenti, E. 1995 *J. Cell Biol.* **129**, 1311.

Cope, F. 1975 *J. Biol. Phys.* **3**, 1.

Cronly-Dillon, J., Carden, D. & Birks, C. 1974 *J. Exp. Biol.* **61**, 443.

Dhamodharan, R., Jordan, M. A., Thrower, D., Wilson, L. & Wadsworth, P. 1995 *Molec. Biol. Cell* **6**, 1215.

Downing, K. 1998 *Nature* **391**, 199.

Dustin, P. 1984 *Microtubules.* Berlin: Springer.

Engelborghs, Y. & Van Houtte, A. 1981 *Biophys. Chem.* **14**, 195.

Feynmann, R. P. 1986 *Found. Phys.* **16**, 507.

Flyvbjerg, H., Holy, T. & Leibler, S. 1994 *Phys. Rev. Lett.* **73**, 2372.

Fukada, E. 1974 *Adv. Biophys.* **6**, 121.

Fukada, E. 1983 *Q. Rev. Biophys.* **16**, 59.

Glanz, J. 1997 *Science* **276**, 678.

Gutmann, F. 1986 *Modern biochemisty.* New York: Plenum.

Hameroff, S. R. 1987 *Ultimate computing.* Amsterdam: North-Holland.

Hameroff, S. R. & Penrose, R. 1996 *J. Consci. Studies* **3**, 36.

Hameroff, S. R., Rasmussen, S. & Mansson, B. 1988 Molecular automata in microtubules: basic computational logic of the living state? In *Artificial life.* New York: Addison-Wesley.

Harris, A. K., Pryer, N. K. & Paydarfar, D. 1990 *J. Exp. Zool.* **253**, 163.

Hasted, J. 1973 *Aqueons dielectrics.* London: Chapman & Hall.

Hirokawa, N. 1991 *Molecular architecture and dynamics of neuronal cytoskeleton.* New York: Wiley.

Hopfield, J. J. 1991 In *Evolutionary trends in physical sciences* (ed. M. Suzuki & R. Kubo). Berlin: Springer.

Horio, T. & Hotani, H. 1986 *Nature* **321**, 605.

Howard, W. & Timasheff, S. 1986 *Biochem.* **25**, 8292.

Hyman, A. A., Chrétien, D., Arnal, I. & Wade, R. H. 1995 *J. Cell. Biol.* **128**, 117.

PHILOSOPHICAL TRANSACTIONS OF THE ROYAL SOCIETY A MATHEMATICAL, PHYSICAL & ENGINEERING SCIENCES

Insinna, E., Zaborski, P. & Tuszyński, J. A. 1996 *Biosystems* **39**, 107.

Jaffe, L. & Nuccitelli, R. 1977 *A. Rev. Biophys. Bioeng.* **6**, 445.

Joshi, H. C. & Cleveland, D. W. 1990 *Cell Motil. Cytoskel.* **16**, 159.

Klauber, N., Payangi, S., Flynn, E., Hamel, E. & D'Amato, R. J. 1997 *Cancer Res.* **57**, 81.

Koruga, D. & Simić-Krstic, J. 1990 *J. Molec. Electr.* **6**, 167.

Li, Y. 1996 & Black, M. 1996 *J. Neuroscience* **16**, 531.

Lieb, E. H. 1995 The Hubbard model: some rigorous results and open problems. In *The Hubbard model*. New York: Plenum.

Mahan, G. D. 1981 *Many-particle physics*. New York: Plenum.

Mandelkow, E. & Mandelkow, E.-M. 1994 *Curr. Opin. Struct. Biol.* **4**, 171.

Mandelkow, E. & Mandelkow, E.-M. 1995 *Curr. Opin. Cell. Biol.* **7**, 72.

Maniotis, A. J., Chen, C. S. & Ingber, D. E. 1997 *Proc. Natn. Acad. Sci. USA* **94**, 849.

Mascarenhas, S. 1974 *Ann. N.Y. Acad. Sci.* **238**, 36.

Mel, B. W. 1994 *Neural Computation* **6**, 1031.

Mickey, B. & Howard, J. 1995 *J. Cell. Biol.* **139**, 909.

Mitchison, T. & Kirschner, M. 1984 *Nature* **312**, 237.

Moskowitz, P. & Oblinger, M. 1995 *J. Neurosci.* **15**, 1545.

Nakamura, H. & Wada, A. 1985 *J. Phys. Soc. Jap.* **54**, 4047.

O'Brien, E. T., Salmon, E. D. & Erickson, H. P. 1997 *Cell Mot. Cytoskel.* **36**, 125.

Pethig, R. 1982 *J. Biol. Phys.* **10**, 201.

Post, J. 1995 *J. Biol. Phys.* **21**, 141.

Pryer, N., Walker, R., Skeen, V., Bourns, B., Soboeiro, M. & Salmon, E. 1992 *J. Cell. Sci.* **103**, 965.

Pullman, B. & Pullman, A. 1962 *Nature* **196**, 1137.

Sackett, D. 1997 *Presentation at the Banff Workshop 'Molecular Biophysics of the Cytoskeleton', August 1997.*

Satarić, M., Tuszyński, J. A. & Žakula, R. 1993 *Phys. Rev.* E **48**, 589.

Schlecht, P. 1969 *Biopolymers* **8**, 757.

Segel, L. A. & Parnas, H. 1991 *Biologically inspired physics* (ed. L. Peliti). New York: Plenum.

Semenov, M. 1996 *J. Theor. Biol.* **179**, 91.

Sirenko, Y. M., Stroscio, M. A. & Kim, K. W. 1996 *Phys. Rev.* E **53**, 1003.

Skoutias, D. A. & Wilson, L. 1992 *Biochem.* **31**, 738.

Sunkel, C. E., Gomes, R., Sampaio, P., Perdigao, J. & Gonzales, C. 1995 *EMBO Jl* **14**, 28.

Trpišova, B. & Tuszyński, J. A. 1997 *Phys. Rev.* E **55**, 3289.

Tsong, T. 1989 *Molecular electronics*. New York: Plenum.

Tuszyński, J. A., Hameroff, S. R., Satarić, M., Trpišová, B. & Nip, M. L. A. 1995 *J. Theor. Biol.* **174**, 371.

Vassilev, P., Dronzine, R., Vassileva, M. & Georgiev, G. 1982 *Biosci. Rep.* **21**, 1025.

Wangermann, G. 1980 *Stud. Biophysica* **132**, 9.

White, R. G., Hyde, G. J. & Overall, R. L. 1990 *Protoplasma* **158**, 73.

Yeomans, J. M. 1992 *Statistical mechanics of phase transitions*. Oxford University Press.

PHILOSOPHICAL TRANSACTIONS OF THE ROYAL SOCIETY A MATHEMATICAL, PHYSICAL & ENGINEERING SCIENCES

Discussion

P. Marcer (*BCS Cybernetic Machine Group, Keynsham, UK*). I believe that no one, with the exception of Professor Zoller, has touched on the fact that computations must concern UNIT WIRE and EXCHANGE primitives as well as ANDs and ORs (as was pointed out by Feynman), or their quantum equivalents. Perhaps, therefore, this is a basic function of the microtubule, particularly as it has been shown that such tubules have two fundamental phases, one conductive and one semiconductive. This would support the Penrose–Hameroff consciousness postulate, which states that this phase transition is pertinent to allowing the transmitted signals to rise to a higher 'quantum' level of awareness via conduction rather than semiconduction until the brain becomes consciously rather than unconsciously aware. The ubiquitous nature of microtubules would also be consonant with this function as a unit wire, as is the case with current technology.

J. A. Tuszyński. I agree with the first part of the statement. We do indeed maintain that microtubules can be suitable semiconducting devices. As much as we have tried to open-mindedly examine, however, we have not found any empirical basis for viewing microtubules quantum mechanically. They certainly play a significant role in the functioning of the brain, but linking them with the emergence of consciousness is in our view somewhat premature.

PHILOSOPHICAL TRANSACTIONS OF THE ROYAL SOCIETY A MATHEMATICAL, PHYSICAL & ENGINEERING SCIENCES